

Fabrication and Characterization of Novel Crosslinked Composite Membranes for Direct Methanol Fuel Cell Application – Part II. Poly (Vinyl Alcohol-Co-Vinyl Acetate-Co-Itaconic Acid)/ Silicotungstic Acid Based Membranes

Arfat Anis^{1,2,*}, S. M. Al-Zahrani¹, A.K. Banthia² and S. Bandyopadhyay³

¹ Dept. of Chemical Engineering, King Saud University, P.O. Box - 800, Riyadh 11421, Saudi Arabia

² Materials Science Centre, Indian Institute of Technology, Kharagpur, India - 721302

³ School of Materials Science & Engineering, University of New South Wales, Sydney 2052, Australia

*E-mail: anisarfath@yahoo.co.in

Received: 30 May 2011 / *Accepted:* 13 June 2011 / *Published:* 1 July 2011

A series of novel cross-linked Poly (vinyl alcohol-co-vinyl acetate-co-itaconic acid) (PVACO) and silicotungstic acid (STA) based organic-inorganic composite membranes have been prepared and characterized for direct methanol fuel cell (DMFC) applications. The characteristic properties of these crosslinked composite membranes were investigated by Fourier transform infrared spectroscopy (FTIR), thermogravimetric analysis (TGA), X-ray diffraction (XRD), Atomic Force Microscopy (AFM), methanol permeability measurement and AC impedance spectroscopy. The ionic conductivity of the membranes were investigated as a function of STA composition, crosslinking density and temperature, were in the order of 10^{-3} S/cm. The methanol permeability of PVACO/STA composite membranes was in the order of 10^{-6} cm²/s. The membrane with the best selectivity was found to have a conductivity of 5.02×10^{-3} S/cm and a methanol permeability of 3.10×10^{-6} cm²/s. These membranes showed an Arrhenius behavior for the variation in conductivity with temperature and their activation

Keywords: Direct methanol fuel cell, composite polymer electrolyte membrane, poly vinyl alcohol copolymer, silicotungstic acid, methanol permeability, heteropolyacids

1. INTRODUCTION

Direct methanol fuel cell (DMFC) is one of the most promising future power sources owing to its simplicity, stable operation at relatively low temperatures and high energy density of the used methanol fuel [1]. Perfluorosulfonate ionomer membranes, such as Nafion membranes from DuPont are the most widely used polymer electrolyte membrane in the present DMFCs. The Nafion membranes are associated with a serious methanol crossover problem due to which methanol

permeates from the anode to the cathode. This methanol crossover causes a loss of fuel and creates a mixed potential at the cathode that decreases the electrochemical performance of these cells. A polymer electrolyte membrane which can mitigate the issue of methanol crossover effectively will help in widespread commercialization of this fuel cell technology.

There has been considerable work on poly(vinyl alcohol) (PVA) based PEMs because PVA has excellent methanol barrier properties due to its dense structure formed by strong intra- and intermolecular hydrogen bonding [2,3]. Hence, PVA-based PEMs with semi-IPN structures have been prepared by blending PVA and polyanion, such as poly(acrylic acid) [4], poly(styrene sulfonic acid-co-maleic acid) [5,6], poly(2-acrylamido-2-methylpropane sulfonic acid) [7,8] and heteropoly acids [9-11]. HPAs are considered as promising materials in the fabrication of organic-inorganic nanocomposite membranes with a PVA matrix [12,13]. Heteropolyacids (HPAs) are strong bronsted acid as well as solid electrolytes [14]. HPAs are generally water soluble and may leach out of the membrane, which might result in decline in cell performance with time. Li and Wang [15,16] have prepared proton-conducting membranes based on PVA with embedded phosphotungstic acid (PWA) and found that the water uptake, proton conductivity, and methanol permeability increased with the PWA content. In order to improve the reagent endurance and thermal stability of PVA/PWA membranes, addition of SiO₂ [17] and chemical crosslinking with glutaraldehyde [10,11] have been employed.

The present work reports the fabrication and characterization of low cost, environment friendly proton conducting composite polymer electrolyte membranes with potential for DMFC application. An environment friendly, biodegradable copolymer of PVA namely Poly (vinyl alcohol-co-vinyl acetate-co-itaconic acid) has been utilized as the polymer matrix and silicotungstic (STA), a heteropolyacid as the dopant for the preparation of chemically crosslinked composite polymer electrolyte membranes. The prepared composite polymer electrolyte membranes have been characterized by various characterization techniques to study their feasibility as possible alternative proton conducting polymer electrolyte membranes for DMFC application. The results reported here indicate an improvement in properties over the previously reported PVACO-PTA composites [11].

2. EXPERIMENTAL

2.1. Preparation of the PVACO-STA composite membrane

Poly (vinyl alcohol-co-vinyl acetate-co-itaconic acid), degree of hydrolysis approx. 97 mole % was obtained from Aldrich, USA. Silicotungstic Acid and Glutaraldehyde (25 % aqueous solution) was obtained from LOBA Chemie Pvt. Ltd., Mumbai, India. The glutaraldehyde (25 % aqueous solution) was diluted to 5 % aqueous solution before being used in the preparation of these composite PEMs, Methanol was obtained from Merck Limited, Mumbai, India. The PVACO-STA crosslinked composite membranes were prepared by a solution casting method. The polymer solution (5 % (w/v)) was prepared by dissolving PVACO in deionized water at 80 °C with continuous stirring until homogeneous and viscous. The required amount of the STA was added to 20 g of the 5 wt % polymer

solution and the resulting mixture was stirred at room temperature (25 °C) until a homogeneous solution was obtained. The required amount of the glutaraldehyde (GA) crosslinking reagent (CLR) was added to the PVACO-STA homogeneous solution and the solution was further stirred for a few minutes to homogenize the solution for accomplishing uniform crosslinking. After this, the solution was poured onto glass petridish and allowed to dry at room temperature for around 48 hours. The dried membranes were peeled off the glass substrate and the obtained membranes were approximately $100 \pm 10 \mu\text{m}$ in thickness.

2.2. Characterization of the PVACO-STA composite membrane

Attenuated Total Reflection (ATR)-FTIR spectra of the pure polymer membranes, pure heteropoly acids and the composite membranes was obtained with a FTIR Spectroscop (NEXUS-870, Thermo Nicolet Corporation) in the range of $4000 - 600 \text{ cm}^{-1}$. Water uptake of the crosslinked pristine polymer membranes and the composite membranes was determined by measuring the change in the weight before and after hydration and titration method was used to determine the dopant loss from the membranes to account for bleeding out of the acids upon hydration.

Conductivity measurements for the PVACO-STA composite membranes were made via the AC impedance method. AC impedance spectra of the membranes were obtained by using Agilent 4294A Precision Impedance Analyzer under an oscillation potential of 10 mV from 40 Hz to 10 MHz at 100 % relative humidity to prevent any moisture loss from the membrane due to desorption during the measurements. The measurement of methanol diffusion co-efficient through the composite membranes was performed using an in house built diffusion cell having two compartments separated by the membrane situated horizontally. The methanol concentration of the receptor compartment was estimated using a differential refractometer (Photal OTSUKA Electronics, DRM-1021); the differential refractometer is highly sensitive to the presence of methanol.

Thermal stability of the composite membranes was studied by thermogravimetric analysis of the pristine polymers and the composite membranes using a NETZSCH TG 209 F1 thermogravimetric analyser. The tensile strength measurement of the composite membranes was carried out using Hounsfield H10KS tensile testing machine. X-ray diffraction patterns for the pristine raw materials and the composite membranes were obtained by using a Phillips X-Pert Diffractometer, using a $\text{Cu-K}\alpha 1$ radiation and operating at 40 kV and 25 mA. Surface morphology of these membranes was studied by atomic force microscopy performed using a Digital Instruments 3000 AFM. The details of these characterization techniques have already been reported in our previous works [10,11].

3. RESULTS AND DISCUSSION

3.1. FTIR Spectroscopy, Water Uptake and Dopant Loss Measurements

The FTIR spectra of the pristine PVACO and glutaraldehyde crosslinked PVACO membranes (PVACO/GA) have been reported and discussed in detail in our previous works [10,11]. The FTIR

spectra of pure STA and the influence of STA addition on the skeletal modes in the PVACO/STA composites is depicted in Fig. 1. The FTIR spectrum of pure STA shows the typical features of Keggin anions. According to the assignments of Rocchiccioli - Deltcheff et al. [18], the four absorption bands at 981, 925, 891, 777 cm^{-1} are assigned to the $\nu(\text{W-O}_t)$ (O_t refers to the terminal oxygen), $\nu(\text{Si-O})$, $\nu(\text{W-O}_e\text{-W})$ (O_e refers to the edge oxygen), and $\nu(\text{W-O}_c\text{-W})$ (O_c refers to the corner oxygen) respectively.

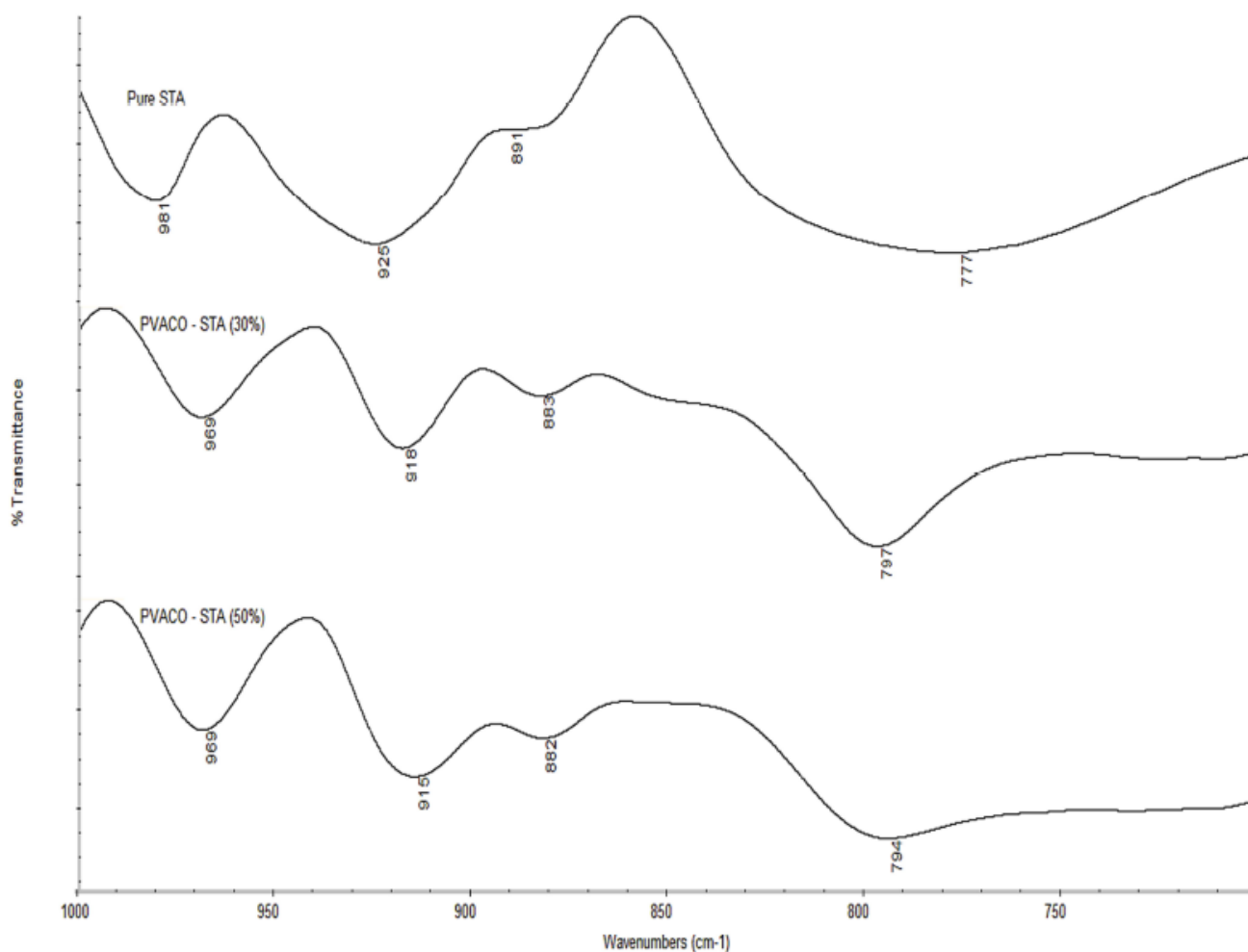


Figure 1. FTIR spectra of Pure STA and glutaraldehyde crosslinked composite membranes with different wt. % STA content and same CLR content (0.5 ml)

All these characteristic bands of STA are also present in the spectra of the composites, indicating the preservation of Keggin ions geometry inside the polymer composites. The most pronounced change, which appears in spectra of the composites, is the shift of the $\text{W-O}_c\text{-W}$ stretching mode peak towards higher wave numbers. The observed effect is stronger for systems with lower acid concentration. Similar behaviour has been observed for many STA containing systems, e.g. for SiO_2 -STA composites [19] or ICS-PPG/STA electrolytes [20] and is due to the increase in the distance between the anions and hence the weakening of dipolar interactions. The increase in the frequency may be explained as a consequence of a mixed, stretching bending character of this vibration. The

bands ascribed to the ν (W-O_t), ν (Si-O) and ν (W-O_e-W) stretching vibrations move to lower frequencies with increase in acid concentration.

The FTIR spectrum in Fig. 2 is associated with PVACO/STA composite membranes crosslinked by glutaraldehyde. This composite membrane shows substantial decrease in the O-H stretching vibration peak ($\nu = 3200\text{-}3500\text{ cm}^{-1}$) when compared to PVACO/GA membrane without STA as reported earlier [11], a weak peak of the C=O band ($\nu = 1640\text{ cm}^{-1}$) indicates that the aldehyde groups of GA have completely reacted with O-H groups of the PVACO chain in the presence of STA which acts as a catalyst for the PVACO-glutaraldehyde crosslinking reaction. In addition, increase in intensity the C-O stretching peaks at $1260, 1190\text{ cm}^{-1}$, can be attributed to the formation of ether (C-O) and the acetal ring (C-O-C) linkages by the crosslinking reaction of PVACO with GA.

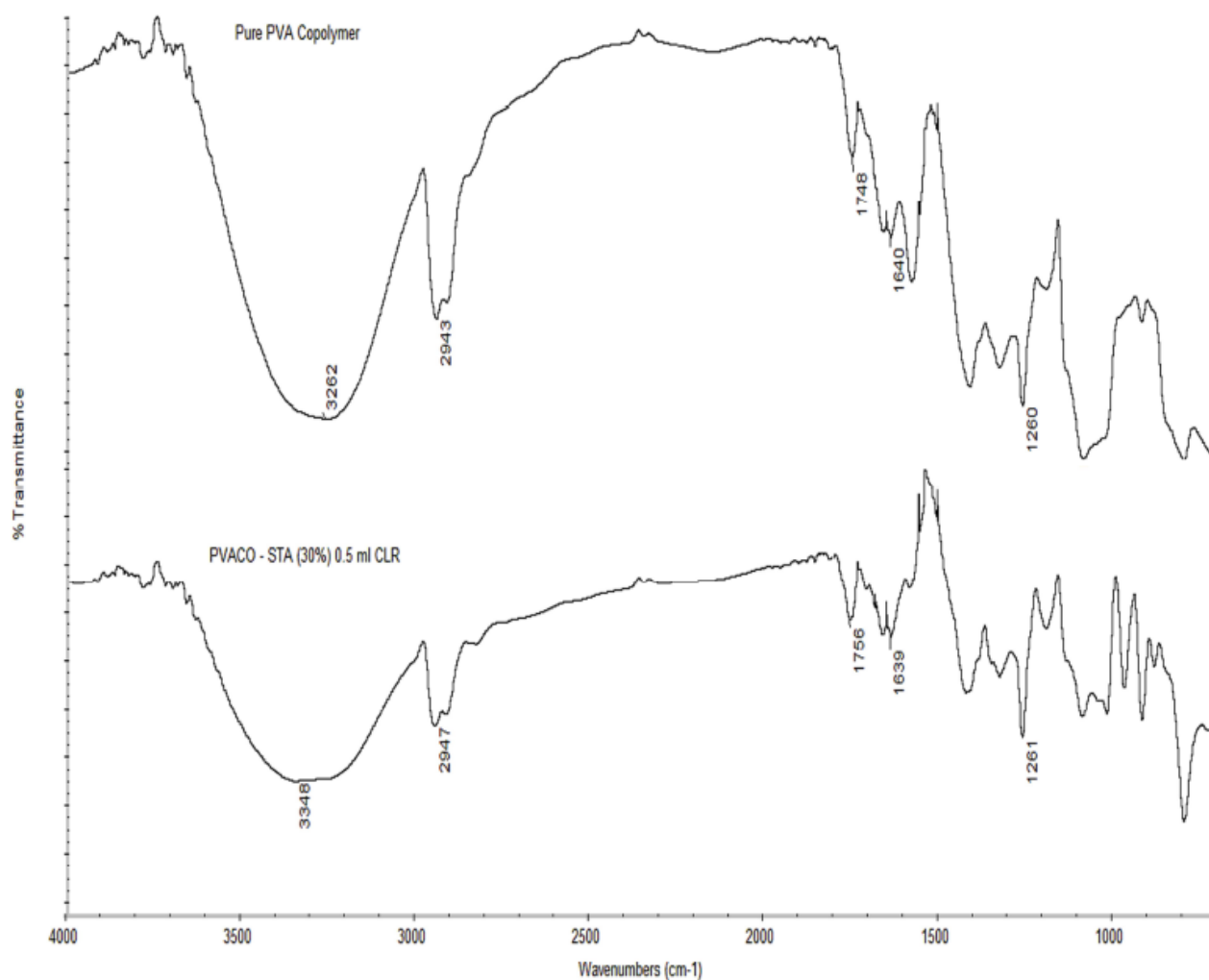


Figure 2. FTIR spectra of Pure PVACO (uncrosslinked) and the glutaraldehyde crosslinked (CLR=0.5 ml) composite membrane with 30 wt. % STA content

The FTIR spectra of the PVACO/STA composite membranes with same weight percent of STA content but with different glutaraldehyde crosslinking reagent (CLR) content are depicted in Fig. 3. The increase in the CLR content of these composite membranes lead to further decrease in the O-H

stretching vibration peak, increase in intensity of the peak (1260 cm^{-1}) and frequency shift of the peak from 1193 to 1189 cm^{-1} associated with the formation of ether (C-O) and the acetal ring (C-O-C) linkages. These observations further confirm the accomplishment of the crosslinking reaction in the prepared PVACO/STA composite membranes.

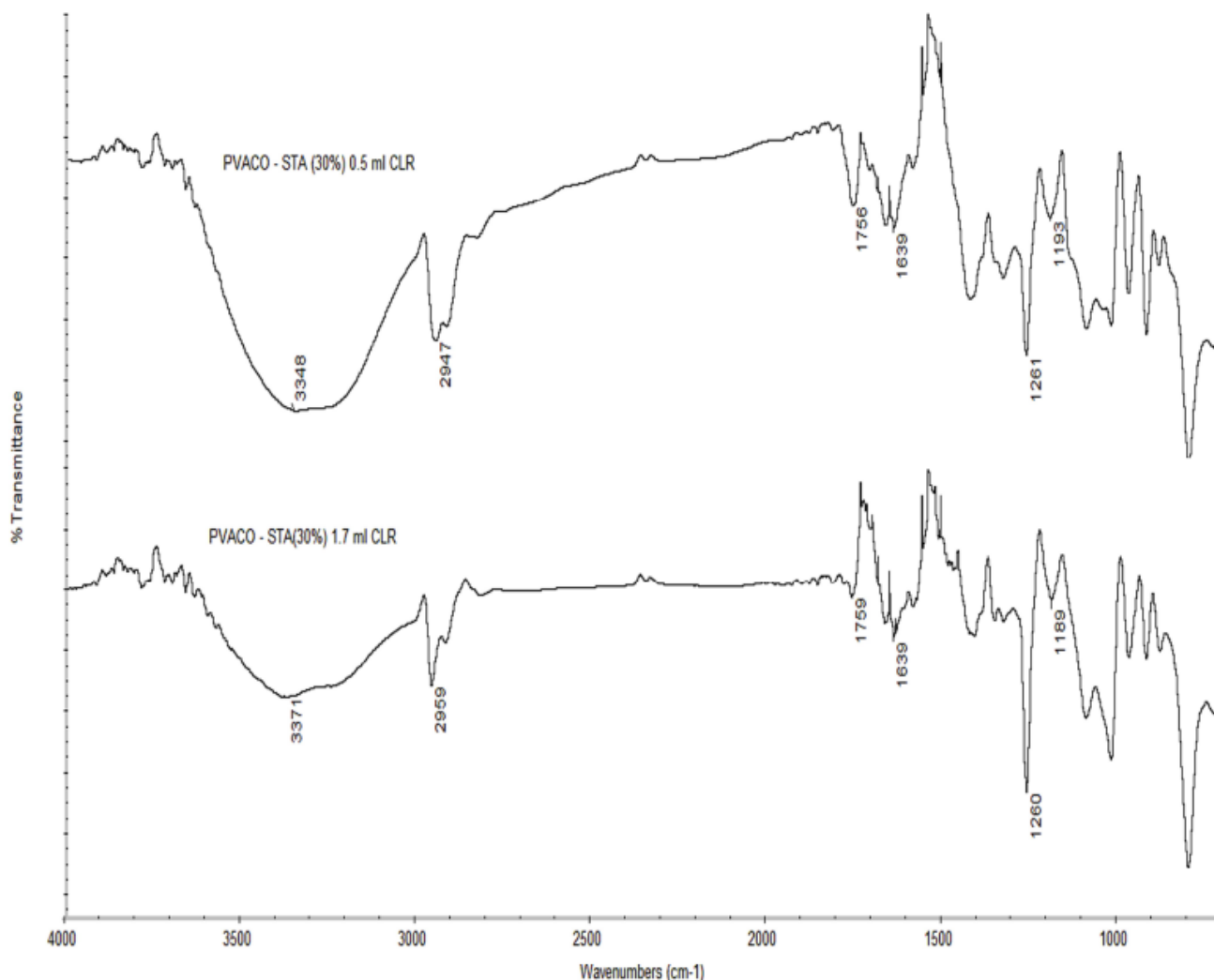


Figure 3. FTIR spectra of crosslinked PVACO/STA composite membranes with constant (30 wt. %) STA content and different (0.5 & 1.7 ml) glutaraldehyde cross linking reagent

The water uptake of the pristine as well as the PVACO/STA composite membranes with different wt. % STA content is shown in Fig. 4. The CLR content was kept constant (0.5 ml) for the preparation of these composite membranes. The pristine membrane showed a very high water uptake of 4.8 gram per gram of the dry polymer, a decrease of around 10 % in the water uptake of the membrane was observed by the incorporation of 10 wt. % of STA in the membrane. When the STA content of the membranes was increased to 30 wt. %, another 12 % decrease in the water uptake of the composite membrane was observed and with further increase in the STA content of the composite membranes to 50 wt. %, a further 85 % decrease in water uptake of the membrane was observed. This

decrease in water uptake of the membranes with increasing STA content is due to the resistance offered by the crosslinked networks, which restrict the swelling and hence the water uptake of the polymer matrix and very well control the hydrophilic character of the composite membranes.

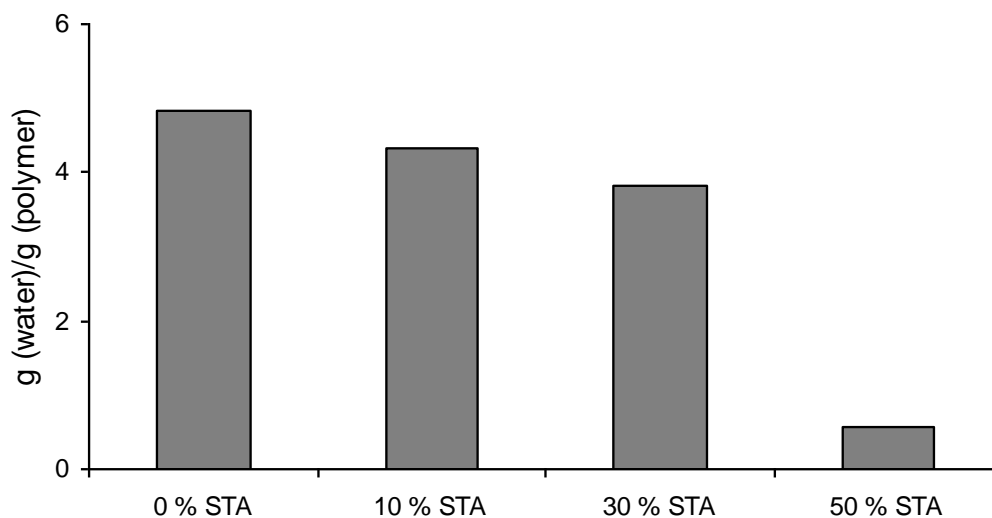


Figure 4. Water Uptake of Crosslinked PVACO membrane (0 wt. % STA, 0.5 ml CLR) and crosslinked composite membranes with different wt. % STA content and constant 0.5 ml glutaraldehyde CLR

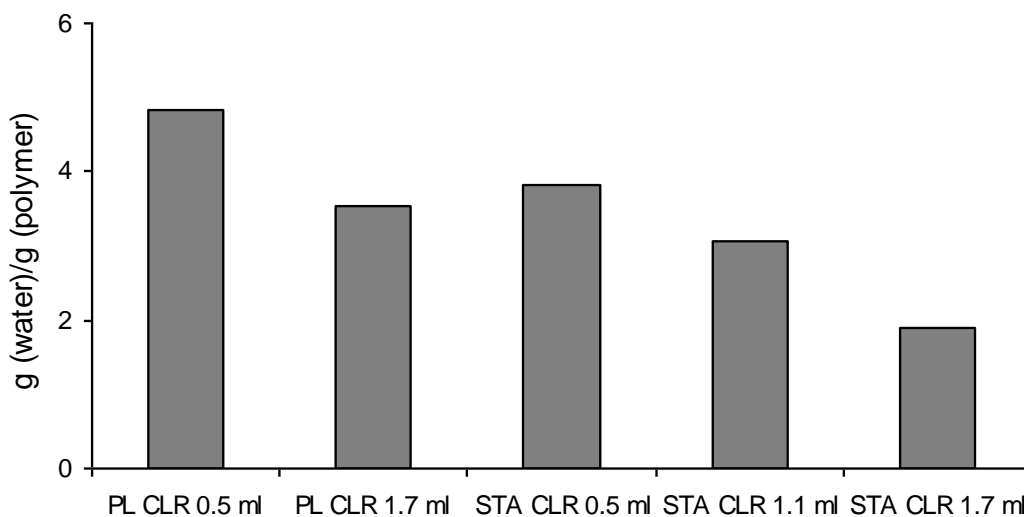


Figure 5. Water Uptake of Crosslinked PVACO (0 wt. % STA) and the crosslinked composite membranes (30 wt. % STA) with different amount of glutaraldehyde cross linking reagent content

The water uptake of the pristine and the PVACO/STA composite membranes (30 wt. % STA content) with different amount of glutaraldehyde CLR content are shown in Fig. 5. The water uptake of the PVACO membrane (without STA) decreases with increase in the cross link density of the membrane. A decrease in water uptake is observed for the composite membrane with 30 wt. % STA

content compared to the membrane without STA but same degree of crosslink density, which further decreases with increase in cross link density of the membranes. The minimum water uptake of 0.56 g/g was observed for the composite membranes with 50 wt. % STA content and 0.5 ml of glutaraldehyde cross linking reagent content.

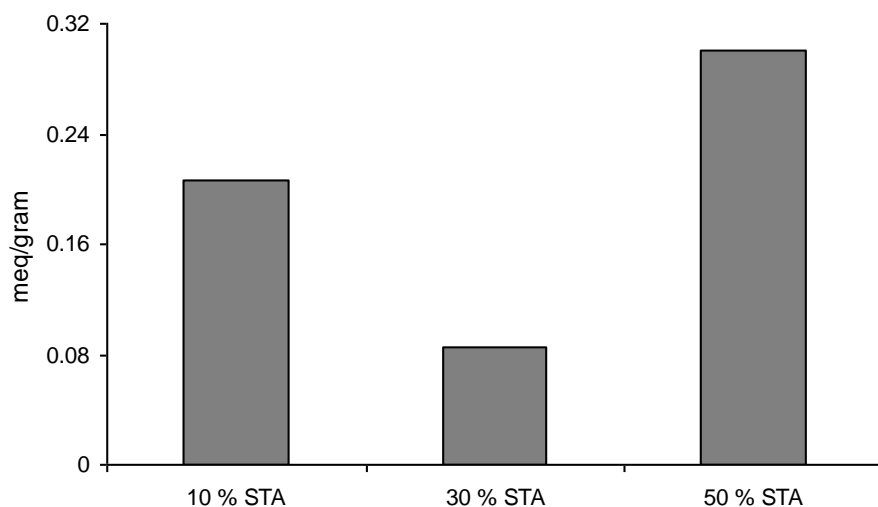


Figure 6. Dopant loss from the crosslinked PVACO-STA composite membranes with (0.5 ml CLR) and different wt. % STA content

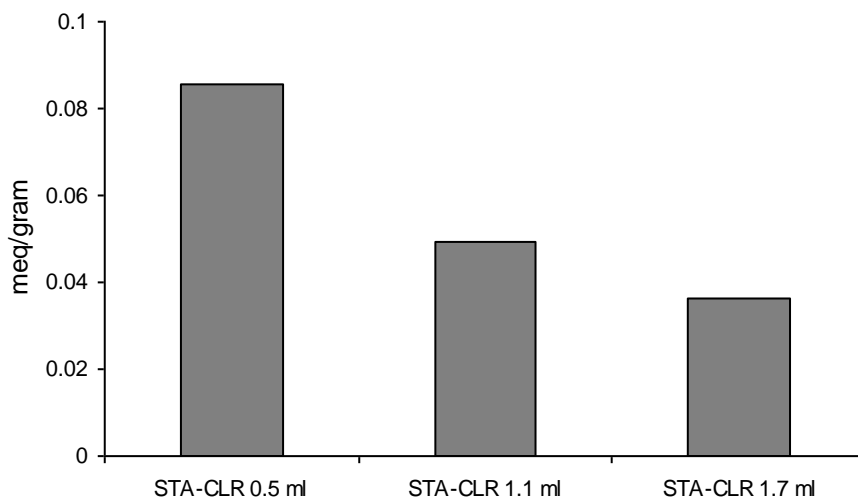


Figure 7. Dopant loss from the crosslinked PVACO-STA composites with 30 wt. % STA and different amount of glutaraldehyde cross linking reagent content

The major problem associated with organic-inorganic composite polymer electrolyte membranes is the bleeding out of dopant from the polymer matrix in fuel cell environment which leads to depleted performance of the membrane with time. We investigated this phenomenon in the present study by determining the dopant loss from the PVACO/STA composite membranes by titration method.

The dopant loss values for the PVACO/STA composite membranes are plotted as a function of wt. % STA content and CLR content of the membranes in Fig. 6 and 7 respectively. It can be seen that the dopant loss for the composite membrane decreases sharply with increase in STA content of the membrane from 10 to 30 wt. % but when the acid content is further increased to 50 wt. % there is a substantial increase in the dopant loss from the composite membrane. The pattern of dopant loss from all the PVACO/STA composite membranes further confirms that increase in percent content of the proton conducting component in the composite membrane is not always desirable. In order to further enhance the immobilization of the STA in the composite membranes the crosslink density of the membranes was increased for the composite membrane with 30 wt. % STA content. It was observed that the dopant loss from the membrane decreased considerably with increase in cross link density of the composite membranes.

3.2. Proton Conductivity and Methanol Permeability Measurements

The proton conductivity values for the cross-linked pristine PVACO membrane as well as the PVACO/STA composite membranes with different wt. % STA content are shown in Fig. 8. The conductivity of the composite membrane is in the order of 10^{-3} S/cm and increased substantially with the incorporation of 10 wt. % STA in the membranes. Further a slight but gradual decrease in the conductivity of the composite membranes is observed with further increase in the STA content of the composite membranes.

The change in room temperature conductivity with variation in cross link density of the pristine as well as the PVACO/STA composite membranes is shown in Fig. 9. The conductivity of the pristine PVACO membrane decreases with increase in crosslink density of the membrane which can be attributed to the fact that water uptake of the membrane decreases with increase in crosslink density of the membrane. The conductivity of the composite membranes decreases with increase in crosslink density of the membranes which can be attributed to the continuous decrease in water uptake of these membranes. The highest room temperature conductivity of 5.02×10^{-3} S/cm among the PVACO-STA based composites was observed for the membrane with 10 wt. % STA and 0.5 ml GA CLR content. Recently, similar results have also been reported by Thanganathan et al. [21] for hybrid membranes containing PVA and poly(tetramethylene oxide) with heteropolyacid as a hydrophilic inorganic modifier. Staiti et al. [22] reported composite PBI membranes with silica supported PWA and SiWA which were thermally stable up to 400 °C. The reported conductivity at the operating condition was around 1.5×10^{-3} S/cm at 150 °C for PWA/SiO₂/PBI and 2.23×10^{-3} S/cm at 160 °C for SiWA/SiO₂/PBI.

Temperature dependence of the conductivity in polymer electrolytes has often been taken as indicative of a particular type of conduction mechanism. The dependence of proton conductivity on temperature follows different types of equations according to different kinds of proton-transport mechanism. Arrhenius Eq. can be used to explain the proton hopping mechanism.

Fig. 10 and 11 show the ionic conductivity of the PVACO/STA composites against the reciprocal absolute temperature, the linear relationship confirms that the variation in conductivity with temperature follows an Arrhenius relationship. For the composite membranes with different wt. %

STA content, the activation energy was initially found to increase from 0.14 eV for 10 wt. % STA content to 0.16 eV for 30 wt. % STA content but with further increase in the STA content to 50 wt. %, no noticeable increase in the activation energy is observed.

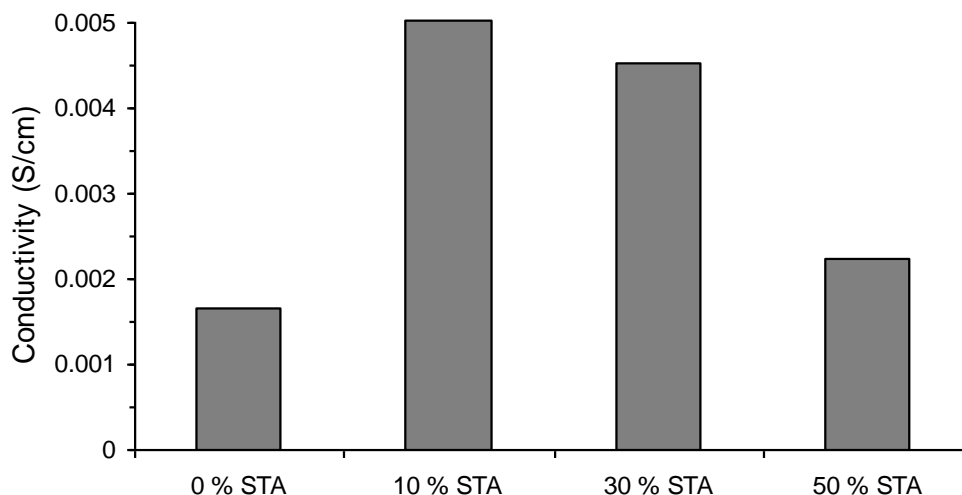


Figure 8. Conductivity of Crosslinked PVACO membrane (0 % STA, 0.5 ml CLR) and crosslinked composite membranes with different wt. % STA content and constant 0.5 ml glutaraldehyde CLR

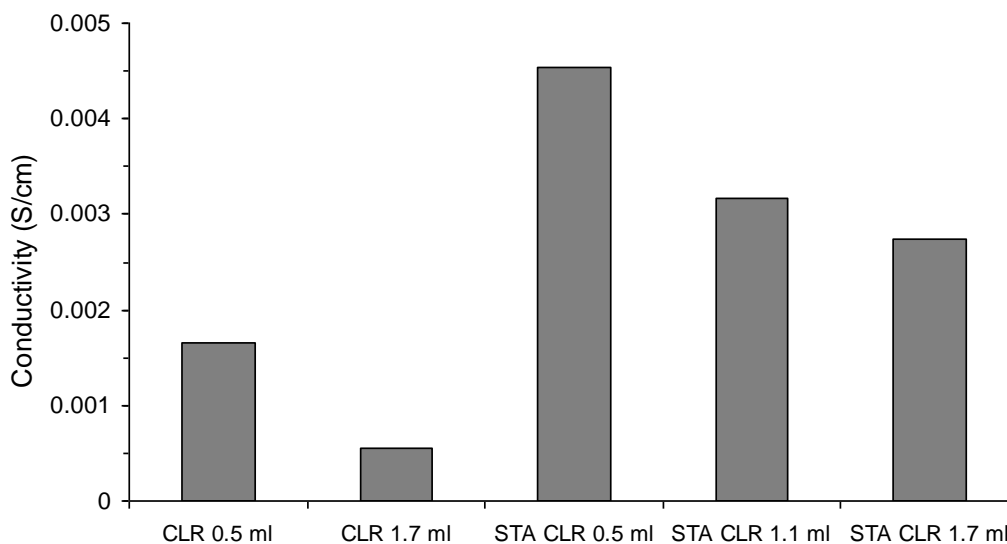


Figure 9. Conductivity of Crosslinked PVACO (0 wt. % STA) and the crosslinked composite membranes (30 wt. % STA) with different amount of glutaraldehyde cross linking reagent

For the composite membranes with 30 wt. % STA content and different CLR content, the activation energy was found to decrease from 0.16 eV to 0.15 eV with increase in CLR from 0.5 ml to 1.7 ml. The variation of conductivity with temperature for all the PVACO/HPA composites follow Arrhenius behavior, therefore it can be suggested that the conductivity is governed by hopping

mechanism in the temperature range of the study. The values of the activation energies for the PEMs are shown in Table 1; the values of the activation energy are much higher than those for pure acids which suggest that the mechanism of the conduction is different from that occurring in the pure acids. Hema et al. [23] have reported similar activation energy of 0.19 eV for a polyvinyl alcohol-ammonium nitrate composite system and also reported that they followed an Arrhenius relationship for temperature dependence of conductivity of these polymer electrolytes.

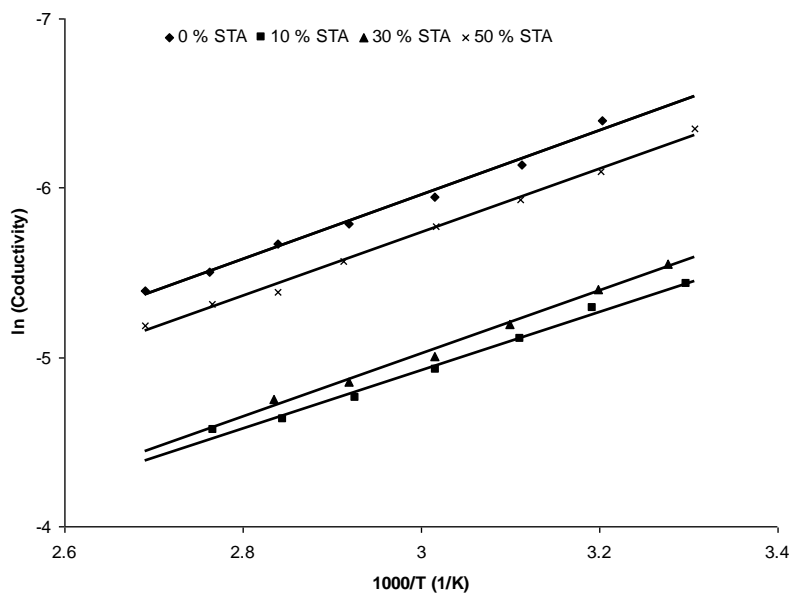


Figure 10. Arrhenius plots for Crosslinked PVACO membrane (0 % STA, 0.5 ml CLR) and crosslinked composite membranes with different wt. % STA content and constant 0.5 ml CLR

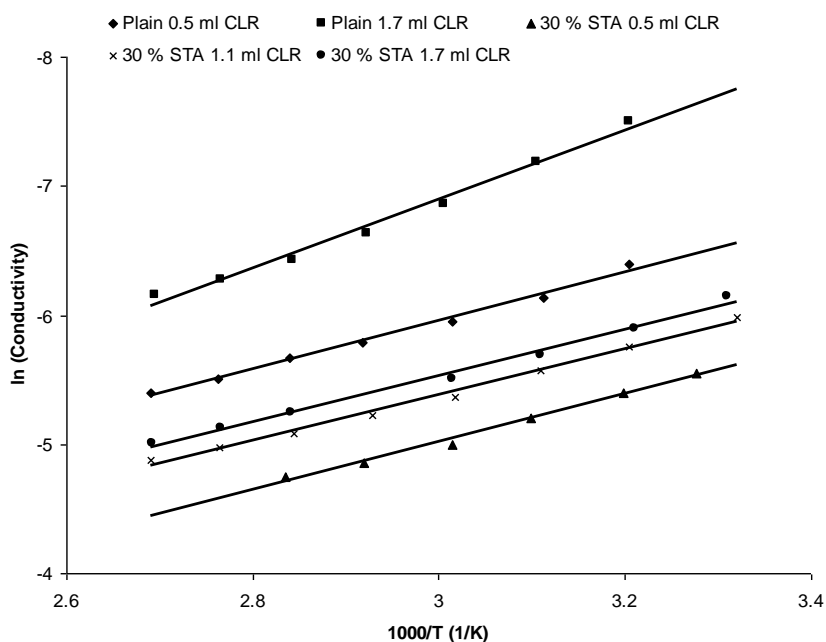
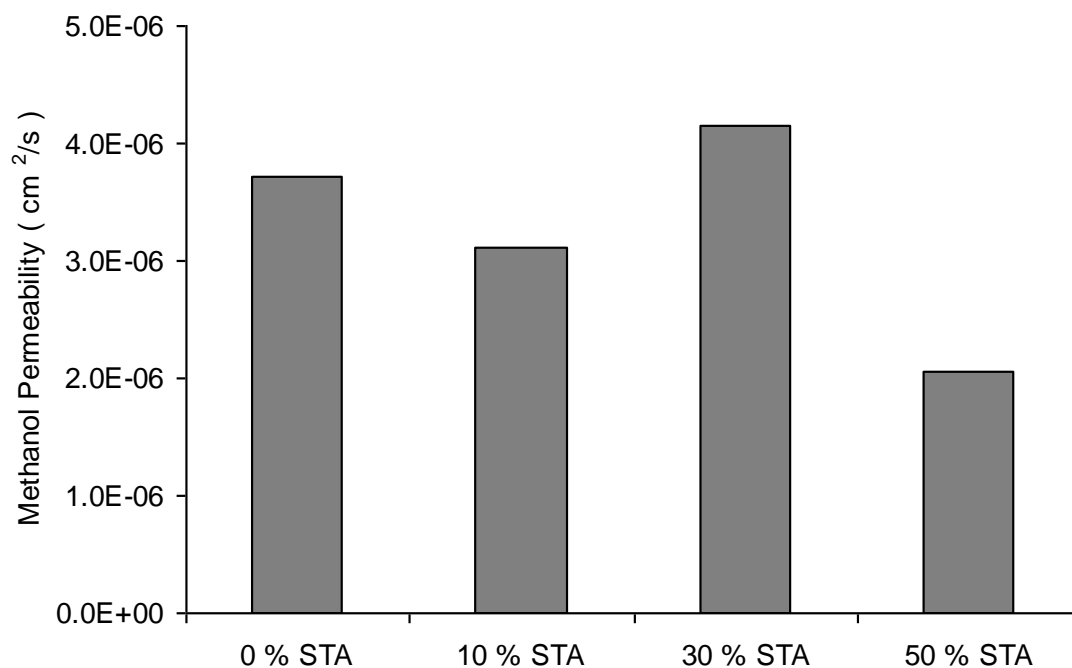


Figure 11. Arrhenius plots for Crosslinked PVACO (0 wt. % STA) and the crosslinked composite membranes (30 wt. % STA) with different amount of glutaraldehyde cross linking reagent

Table 1. R-Squared and Activation Energy values for the Arrhenius plots of the Crosslinked Pure PVACO membranes and the PVACO/STA crosslinked composite membranes

Membrane Details	R ² Value (line fitting)	Activation Energy (eV)
PVACO / 0 wt. % STA / CLR 0.5 ml	0.99	0.16
PVACO / 0 wt. % STA / CLR 1.7 ml	0.98	0.23
PVACO / 10 wt. % STA / CLR 0.5 ml	0.99	0.15
PVACO / 30 wt. % STA / CLR 0.5 ml	0.99	0.16
PVACO / 30 wt. % STA / CLR 1.1 ml	0.99	0.15
PVACO / 30 wt. % STA / CLR 1.7 ml	0.99	0.15
PVACO / 50 wt. % STA / CLR 0.5 ml	0.99	0.16

The methanol permeability of the PVACO/STA composite membranes with different STA content is shown in Fig. 12. The composite membranes with different STA content in general show lower methanol permeability compared to the pristine PVACO membrane. A reduction of more than 15 % was observed in the methanol permeability of the composite membrane by the incorporation of 10 wt. % of STA in the membranes, when the STA content of the membranes was further increased to 30 wt. % a slight increase in the methanol permeability of the composite membrane was observed. With further increase in the STA content of the composite membrane to 50 wt. % a substantial decrease in methanol permeability of the membrane was observed.

**Figure 12.** Methanol permeability of Crosslinked PVACO membrane (0 % STA, 0.5 ml CLR) and crosslinked composite membranes with different wt. % STA content and constant 0.5 ml CLR

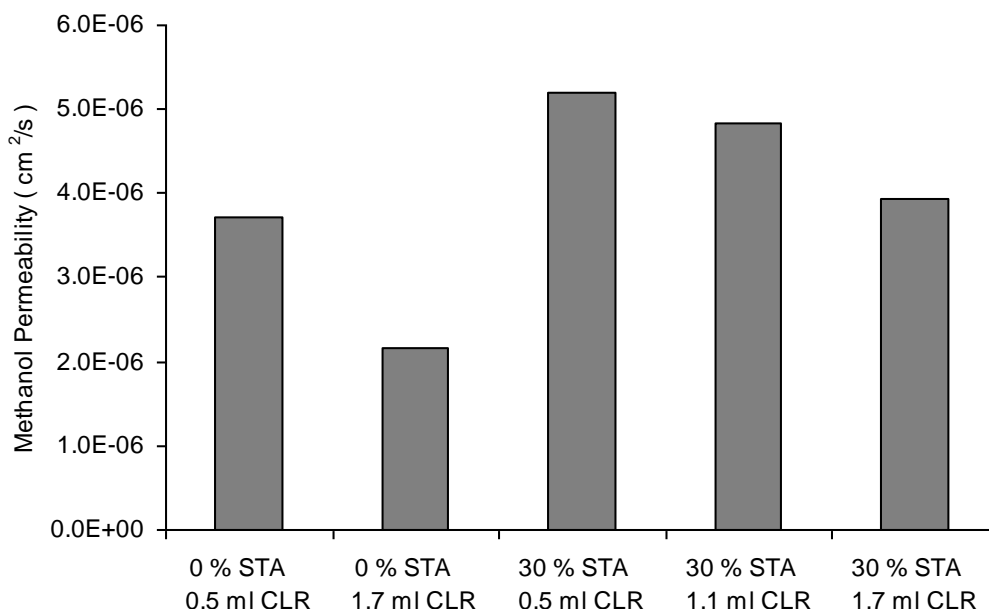


Figure 13. Methanol permeability of Crosslinked PVACO (0 wt. % STA) and the crosslinked composite membranes (30 wt. % STA) with different amount of glutaraldehyde cross linking reagent

Fig. 13 shows the methanol permeability of the pristine and composite membranes (30 % STA content) with different CLR content. The methanol permeability of the PVACO membrane (without STA) decreases with increase in the crosslink density of the membrane. A decrease in methanol permeability is observed for the composite membrane with 30% STA content with increase in cross link density of the membranes but it is always greater than that for the crosslinked pristine PVACO membranes. The minimum methanol permeability of $2.06 \times 10^{-6} \text{ cm}^2/\text{s}$ was observed for the composite membrane with 50 % STA content and 0.5 ml of glutaraldehyde cross linking reagent. Recently Thomassin et al. [24] reported the addition of Cloisite Na⁺ and phosphotungstic acid to PVA and found that these additives have important influence on both the methanol permeability and ionic conductivity of the composites. Cloisite Na⁺ was found to have a beneficial impact on the methanol permeability and a negative impact on the ionic conductivity, whereas the opposite effect was observed for the addition of phosphotungstic acid.

3.3. Thermal, Mechanical and Morphological properties

The thermal stability of the PVACO/STA composite membranes with different STA content and crosslink density was investigated by thermo gravimetric analysis. The TGA thermograms of the PVACO/STA composites are showed in Fig. 14 and the actual percent weight loss are reported in Table 2. The pristine PVACO is thermally stable up to 230 °C. It can be seen that three consecutive weight loss steps are observed for the PVACO/STA composite membranes. Each weight loss step is responsible for a thermal solvation, thermal degradation of the cross links (ester and ether linkages) and finally a thermal oxidation of the polymer chain respectively. The PVACO/STA composite

membranes show enhanced thermal stability and the composite membrane shows first major weight loss centred around 180 °C. This corresponds to weight loss of absorbed water, structural water associated with STA and water as by-product by further esterification in the PVACO/STA membranes. The second weight loss is centred around 250-450 °C is due to the thermal degradation of the ether and ester crosslinking linkages. The third weight loss is due to degradation of the polymer backbone and/or reaction with air, which starts at around 600 °C. The crosslinked PVACO/STA composite membranes showed considerably enhanced thermal stability than that of the pristine PVACO membranes. Recently it has been demonstrated that silicotungstic acid and PVA composite membranes prepared via sol-gel technique offer good thermally stability at high temperature [25].

Table 2. Percent Weight Loss for the Pristine PVACO and the PVACO/STA composite membranes

Membrane Details	30-200 °C	200-350 °C	350-700 °C	Residue (700 °C)
Pure PVACO	15 %	47 %	27 %	11 %
PVACO/30%STA/0.5mlCLR	09 %	24 %	36 %	31 %
PVACO/30%STA/1.7mlCLR	24 %	12 %	09 %	55 %
PVACO/50%STA/0.5mlCLR	20 %	12 %	10 %	58 %

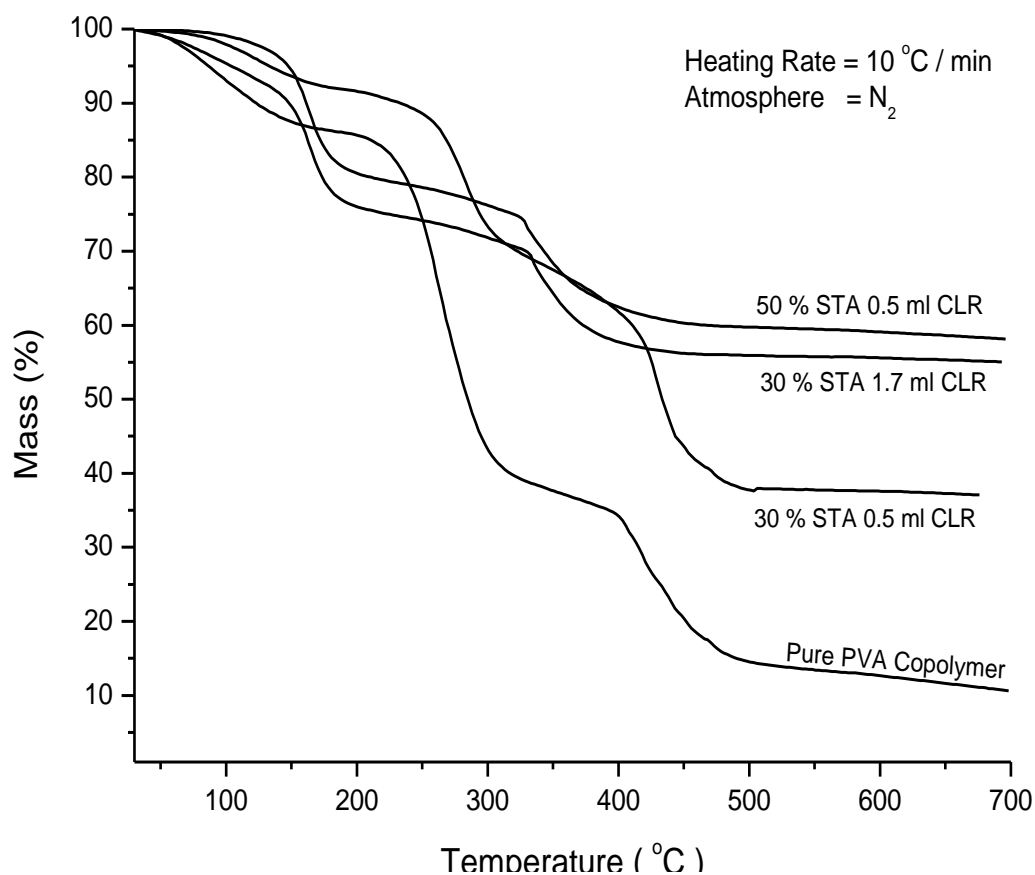


Figure 14. TGA thermograms of Pure PVACO (Uncrosslinked) & Crosslinked PVACO/STA composite membranes with different wt. % STA and glutaraldehyde CLR content

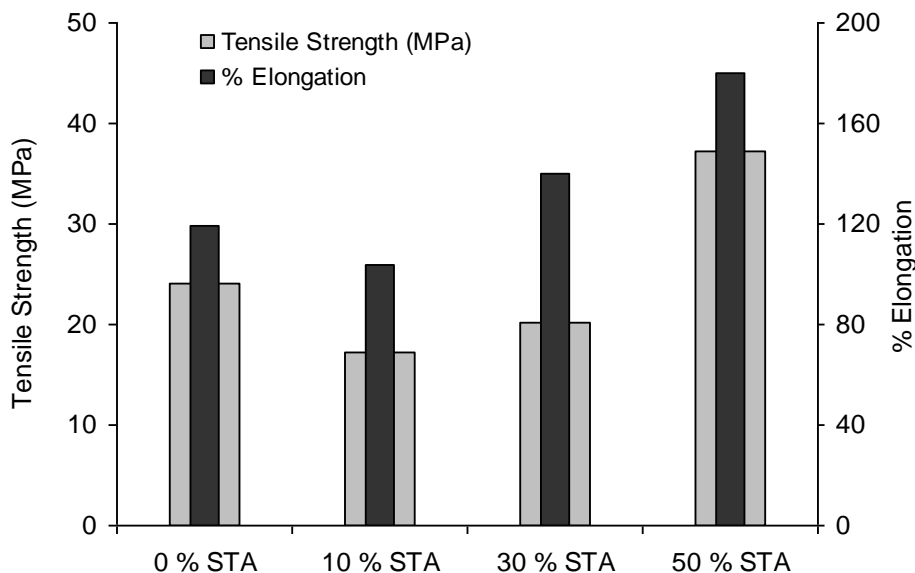


Figure 15. Mechanical properties of the Pristine PVACO and PVACO/STA composite membranes with different STA content and same CLR content of 0.5 ml

The tensile strength and percent elongation at break for PVACO/STA composite membranes with different STA content and cross-link density are shown in Fig. 15 and 16 respectively. The tensile strength for the composite membrane initially decreases with the incorporation of STA in the crosslinked pristine PVACO membranes but increases with further increase in the STA content of the membrane. A similar behavior of an initial decrease and then continuous increase in the percent elongation is observed for the PVACO/STA composite polymer electrolyte membranes.

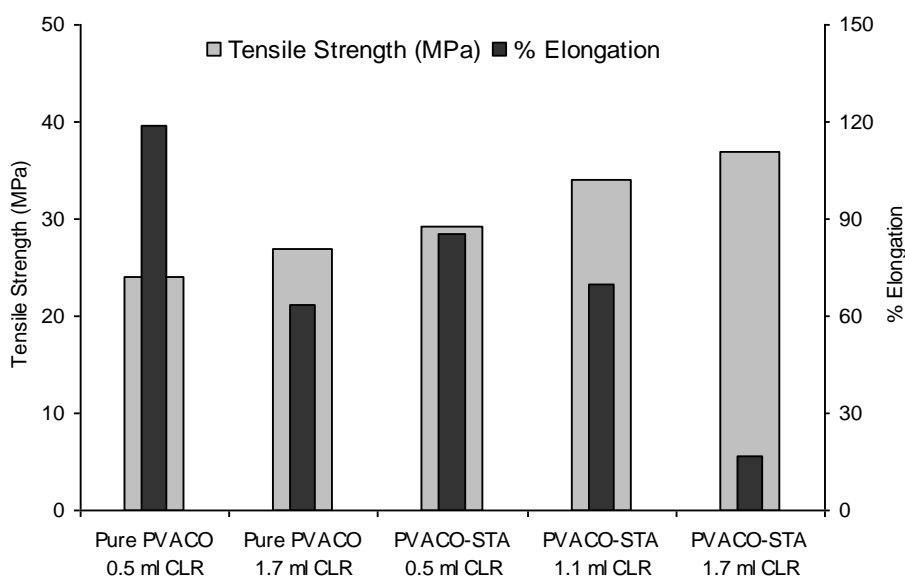


Figure 16. Mechanical properties of the Pristine PVACO and PVACO/STA composite membranes with 30 wt. % STA content and different CLR content

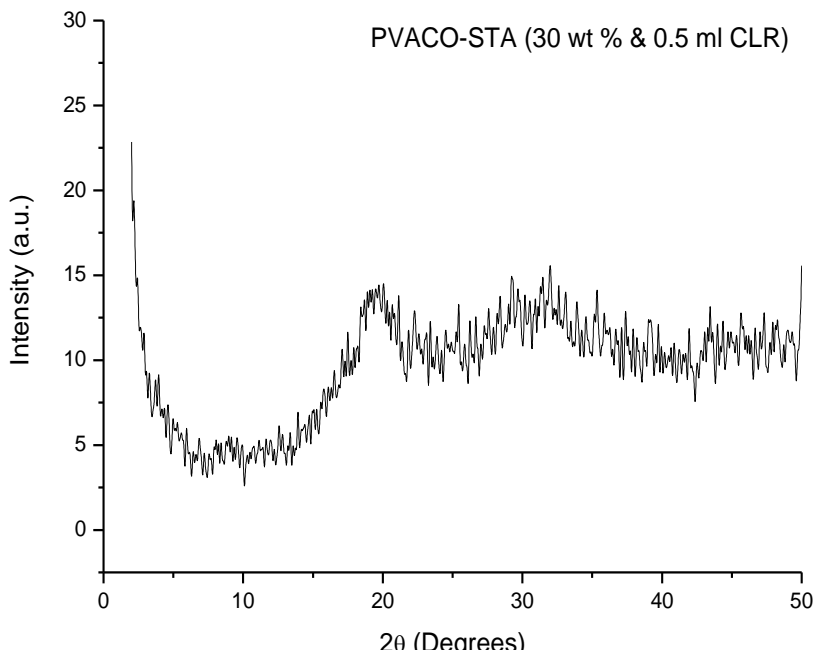


Figure17. X-ray Diffraction pattern of PVACO-STA Composite Membranes (30 wt. % STA and 0.5 ml CLR)

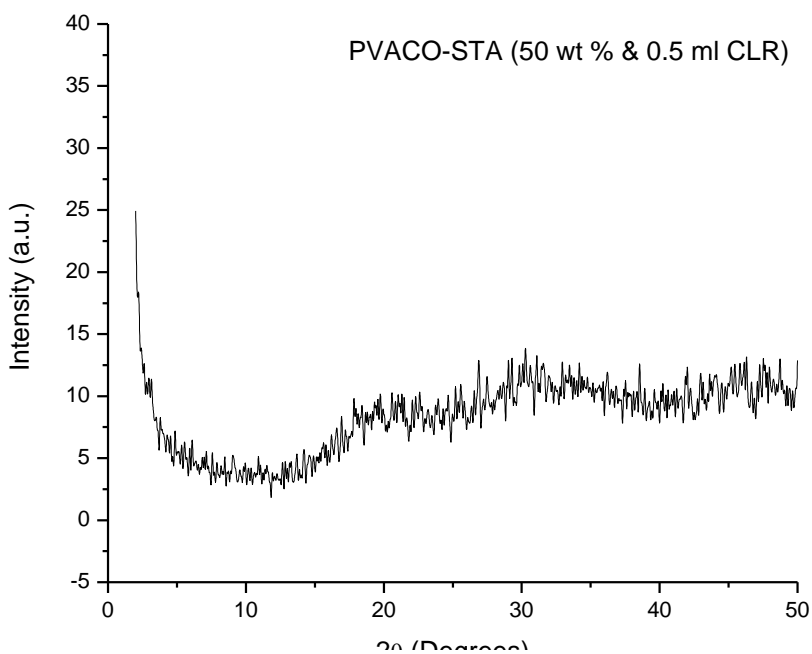


Figure 18. X-ray Diffraction pattern of PVACO-STA Composite Membranes (50 wt. % STA and 0.5 ml CLR)

The tensile strength of the PVACO/STA composite membranes with different CLR content increases with increase in CLR content of the membranes whereas the percent elongation at break decreases with increase in cross-link density of the membrane. From the results it can be observed that

the crosslinked membranes exhibit higher tensile strength than the pristine PVACO. This enhancement in tensile strength and decrease in percent elongation is due to the formation of crosslinked networks hence restricted mobility of the polymer chains.

X-ray diffraction analysis of Pristine PVACO (Uncrosslinked and Crosslinked) and the PVACO/STA composites membranes were performed. The XRD patterns for the Uncrosslinked and Crosslinked Pristine PVACO has been reported earlier [11], the PVACO/STA composite membranes are depicted in Fig. 17 - 18. The range of the diffraction angle $2\theta = 2 - 50^\circ$. The crystallinity of the composite membranes is mainly due to PVACO. There is considerable broadening in the XRD peaks due to STA in the PVACO-STA composite membranes. This feature indicates the reduction in the crystallinity of the composite membranes with increase in STA content of the membranes. The reduction in crystallinity of the composite membranes plays an important role in increasing the conductivity of the composite membranes.

The surface morphology of the Pure PVACO membranes and the PVACO/STA composite membranes were analysed by Tapping Mode - Atomic Force Microscopy (TM-AFM). The TM-AFM image of the uncrosslinked and cross-linked Pure PVACO membrane has been reported earlier [11] and was observed that the morphology of the pure polymer surface changed significantly after cross-linking.

Table 3. Roughness parameters for Pristine PVACO and PVACO/STA composite membrane surfaces

Membrane Details	R_a (nm)	R_{max} (nm)	R_q (nm)
Pure PVACO (Uncrosslinked)	3.06	108.30	5.46
PVACO 1.7 ml CLR (0 % STA)	0.73	15.45	0.97
30 % STA 0.5 ml CLR	1.99	34.17	2.55
50 % STA 0.5 ml CLR	20.75	181.3	25.97
30 % STA 1.7 ml CLR	9.70	148.55	13.05

The composite membrane with 30 wt. % STA content (Fig. 19) shows a homogeneous and non-porous morphology but the surface morphology shows a substantial change with increase of STA content of the composite membranes to 50 wt. % (Fig. 20). The mean roughness for the surface topography of the membrane increases from 1.99 nm to 20.75 nm with increase in STA content of the composite membranes from 30 to 50 wt %. This shows that the heteropoly acid tends to form bigger aggregated particles with increase in the acid content of the composite membranes. When the crosslink density of the composite membrane with 30 wt. % STA content is increased from 0.5 to 1.7 ml CLR (Fig. 21) then the mean roughness of the surface of the membrane increased from 1.99 nm to 9.70 nm.

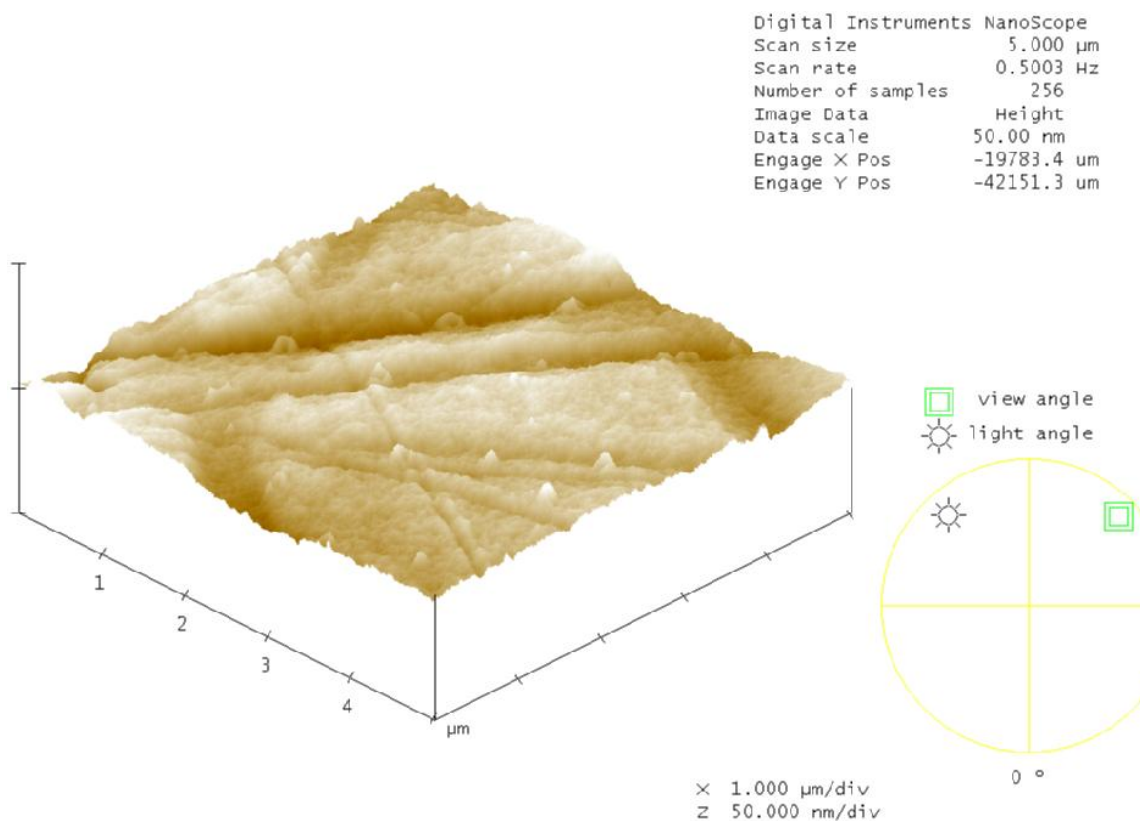


Figure 19. Tapping Mode (3D) AFM images of PVACO-STA composite (30 % STA, 0.5 ml CLR)

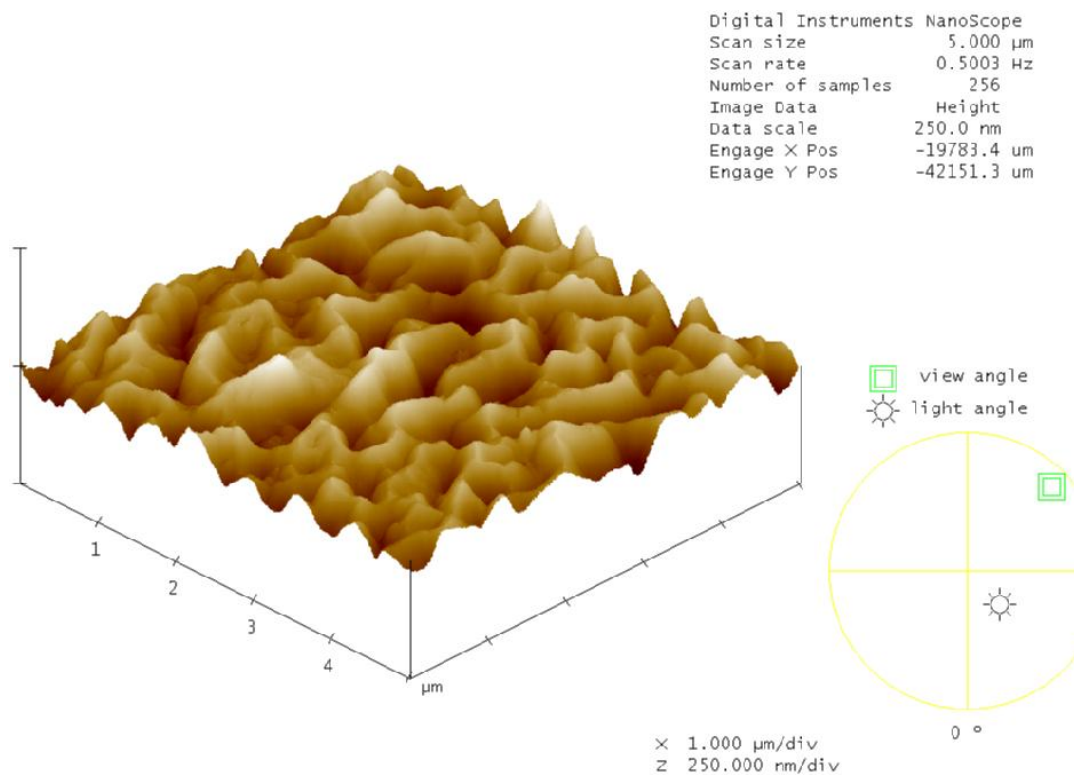


Figure 20. Tapping Mode (3D) AFM images of PVACO-STA composite (50 % STA, 0.5 ml CLR)

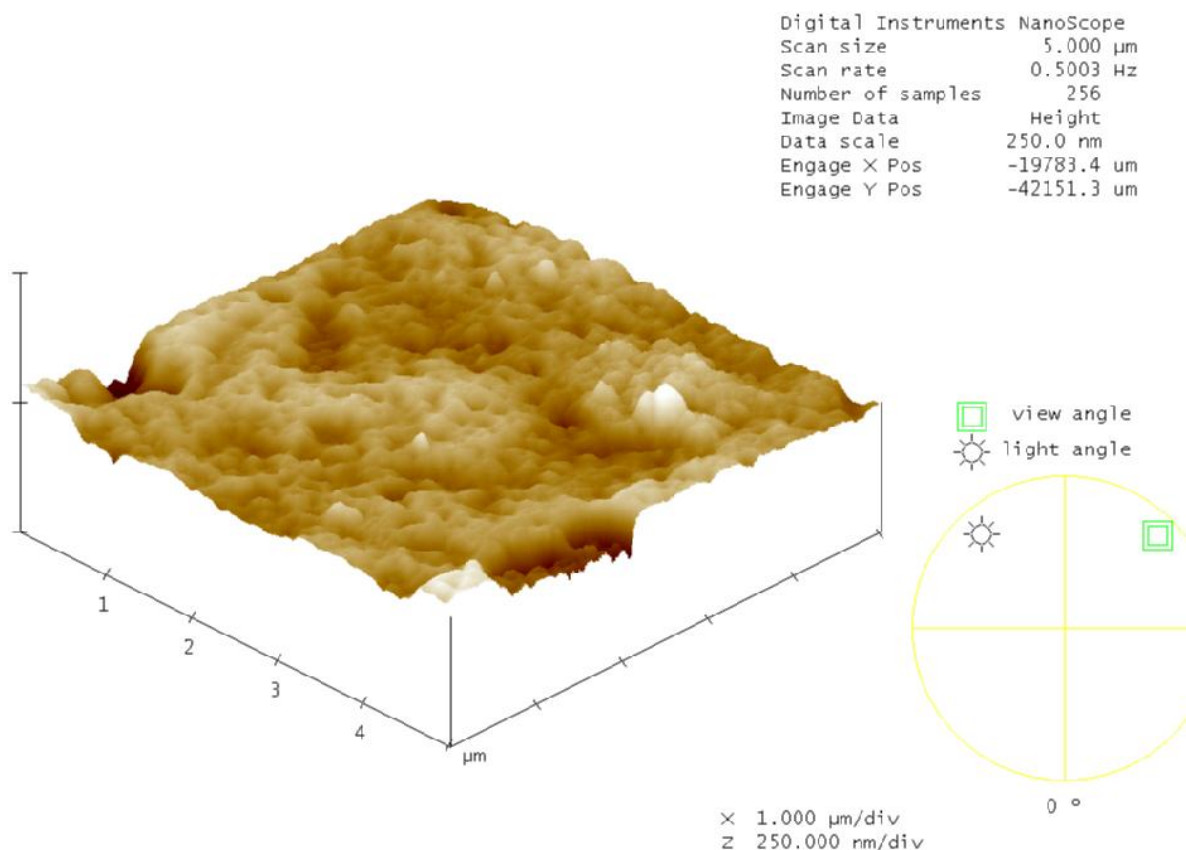


Figure 21. Tapping Mode (3D) AFM images of PVACO-STA composite (30 % STA, 1.7 ml CLR)

4. CONCLUSION

This work reports the fabrication and characterization of PVACO-STA based crosslinked composites by various characterization techniques. The FTIR studies confirmed the formation of crosslinked networks and the occurrence of strong interaction of the heteropoly acids with the hydroxyl and carboxylic acid groups of the PVACO polymer matrix through the terminal and bridging oxygen atoms, which helps in immobilizing the STA in the PVACO polymer matrix. The water uptake and the dopant loss from the composite membranes can be controlled by optimizing the STA content and the crosslink density of the composite membranes. The optimum membrane property among the PVACO-STA composites was observed for the membrane with 10 wt. % STA and 0.5 ml GA CLR, a conductivity of 5.02×10^{-3} S/cm and a methanol permeability of 3.10×10^{-6} cm²/s was observed for this PEM. The variation in conductivity with temperature follows an Arrhenius relationship and the values of activation energy for proton conduction in the PVACO-STA composite membranes ranges were mostly around 0.15 and 0.16 eV as determined from the Arrhenius plots. Improvement in thermal and mechanical properties of the PVACO-STA composites was observed with the incorporation of STA in the PVACO polymer matrix and crosslinking of the polymer matrix respectively. X-Ray diffraction studies showed decrease in crystallinity of the composite membranes which plays an important role in enhancing the proton conductivity of the composite membranes. All the PVACO-STA composite

membranes showed very smooth surface morphology as observed by the AFM except for the composite membrane with the highest (50 wt %) acid content.

ACKNOWLEDGEMENTS

The authors wish to thank the Australia-India Council, Canberra for providing partial funding to enable visiting fellow Dr. Arfat Anis to work at University of New South Wales, Sydney, Australia.

References

1. M. Higa, M. Sugita, S. Maesowa and N. Endo, *Electrochimica Acta*, 55 (2010) 1445
2. T. Hamaay, S. Inoue, J. Qiao and T. Okada, *J. Power Sources*, 156 (2006) 311
3. W.Y. Chiang and C.M. Hu, *J. Appl. Polym. Sci.*, 43 (1991) 2005
4. D.S. Kim, H.B. Park, J.W. Rhim and Y.M. Lee, *Solid State Ionics*, 176 (2005) 117
5. M.S. Kang, J.H. Kim, J. Won, S.H. Moon and Y.S. Kang, *J. Membr. Sci.*, 247 (2005) 127
6. D.S. Kim, M.D. Guiver, S.Y. Nam, T.I. Yun, M.Y. Seo, S.J. Kim, H.S. Hwang and J.W. Rhim, *J. Membr. Sci.*, 281 (2006) 156
7. J. Qiao, T. Hamaay and T. Okada, *J. Mater. Chem.*, 15 (2005) 4414
8. J. Qiao, T. Hamaya and T. Okada, *Polymer*, 46 (2005) 10809
9. C.W. Lin, R. Thangamuthu and C.J. Yang, *J. Membr. Sci.*, 253 (2005) 23
10. A. Anis, A.K. Banthia and S. Bandyopadhyay, *J. of Power Sources*, 179 (2008) 69
11. A. Anis, S.M. Al-Zahrani, A.K. Banthia and S. Bandyopadhyay, *Int. J. Electrochem. Sci.*, 6 (2011) xx
12. B.P. Tripathi and V.K. Shahi, *Progress in Polymer Science*, 36 (2011) 945
13. S. Shanmugam, B. Viswanathan and T.K. Varadarajan, *J. Membr. Sci.*, 275 (2006) 105
14. M. Misono, *Catal. Rev. Sci. Eng.*, 29 (1987) 269
15. L. Li and Y. Wang, *Chin. J. Chem. Eng.*, 10 (2002) 614
16. L. Li, L. Xu and Y.X. Wang, *Mater. Lett.*, 57 (2003) 1406
17. W. Xu, C. Liu, X. Xue, Y. Su, Y. Lv, W. Xing and T. Lu, *Solid State Ionics*, 171 (2004) 121
18. C.R. Deltcheff, M. Fournier, R. Franck and R. Thouvenot, *Inorg. Chem.*, 22 (1983) 207
19. P. Staiti, S. Freni and S. Hocevar, *J. Power Sources*, 79 (1999) 250
20. I. Honma, S. Nomura and H. Nakajima, *J. Membrane Science*, 185 (2001) 83
21. U. Thanganathan, J. Parrondo and B. Rambabu, *J. Appl Electrochem*, 41 (2011) 617
22. P. Staiti, M. Minutoli and S. Hocevar, *J. Power Sources*, 90 (2000) 231
23. M. Hema, S. Selvasekarapandian, H. Nithya, A. Sakunthala and D. Arunkumar, *Ionics*, 15 (2009) 487
24. J.M. Thomassin, C. Pagnouille, G. Caldarella, A. Germain, R. Jerome, *J. Memb. Sci.*, 270 (2006) 50
25. S. Shanmugam, B. Viswanathan and T.K. Varadarajan, *J. Membr. Sci.*, 275 (2006) 105